

# Simulating 3-Dimensional Deep X-ray Lithography Using the CXrL Toolset

G. Aigeldinger<sup>\*,\*\*</sup>, B. Craft<sup>\*</sup> and W. Menz<sup>\*\*</sup>

<sup>\*</sup>Center for Advanced Microstructures and Devices, CAMD, Louisiana State University, Baton Rouge, 70803 Louisiana, USA

<sup>\*\*</sup>Institut für Mikrosystemtechnik, Univ. Freiburg, Germany

## ABSTRACT

Experimental evaluation of the dose distribution resulting from 3-dimensional deep x-ray lithography is often impractical. Computer modeling is a valuable tool for simulating this system.

Preliminary simulations of 3-dimensional, deep, x-ray lithography exposures have been performed using the CXrL Toolset [2]. External computer programs have been developed to allow various manipulations of the resist volume between successive exposures. The first pair of routines allow a cubic volume of resist to be rotated by 90 degrees about either of two orthogonal axes. These have been used to simulate the exposures required to generate a "six-way cross". First experiments producing a six-way cross have been conducted at the NSLS.

The second set of routines supports the simulation of exposures where the x-rays enter the resist at non-normal incidence. A "valve seat" with the geometry of a truncated pyramid has been simulated.

**Keywords:** lithography, simulation, 3-dimensional, x-ray, synchrotron

## INTRODUCTION

The planning of exposure sequences for the fabrication of 3-dimensional structures is a complex problem. Following multiple exposures using various orientations of the resist and different masks, the distribution of dose within the resist is a scalar function of three variables, the spatial coordinates.

The dose can be calculated at any point in the resist after each of the multiple exposures. Modeling also allows for investigation of the evolution of the geometry of the dose distribution which is particularly useful when planning the mask/orientation sequence.

The preliminary simulations were performed to get informations about difficulties encountered with resist data manipulation and storage. The goal was also to investigate possibilities and problems regarding resist re-orientation, compute time, and hardware demands.

## THE SIX-WAY-CROSS

### The CXrL Toolset

The simulations of 3-dimensional lithography were begun with modeling a six-way-cross. The main reason for this lies in the character of the CXrL Toolset which was used to calculate the basic dose deposition in the samples worked on. The Toolset provides a powerful tool for calculating dose distribution dependent on the source, mask and resist of a given lithography problem. The resist and the other components of the system are represented as a number of layers producing a well-defined transmission/absorption problem. All layers, particularly the resist, can be sliced into an arbitrary number of planes. These planes carry a user defined grid. Utilizing a square grid and slicing the resist with the appropriate number of planes results in a cube of uniform cubic voxels. Figure 1 shows the basic representation of a simulated exposure in the Toolset including the cubic resist volume.

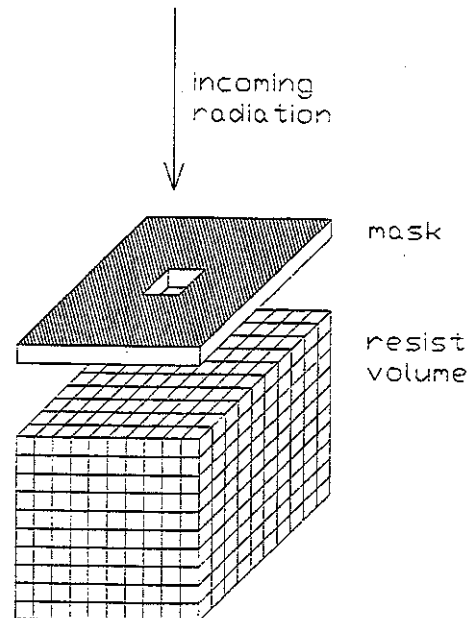


Figure 1: Basic representation of an exposure system in the CXrL Toolset.

There are 24 distinct orientations of the cubic resist volume that leave the material properties of the system unchanged. This group of discrete rotations can be covered using two generators. Specifically, two 90 degree rotations about orthogonal axes were used. The six-way cross is simulated by using an appropriate sequence of exposures and these two rotations.

Another reason why the six-way cross has been chosen is because it is a good structure to characterize a sample-manipulator/mask-aligner combination. The alignment of all manipulator axes and mask aperture relative to each other can be verified analyzing the resulting structure. Realignment can be done based on the results from the six-way cross sample. As the square aperture in the mask is decreased in size, the alignment tolerances of the system must be decreased to maintain intersection of the three tubes.

### External Programs for Resist Manipulation

Following an exposure run, the Toolset can produce an ASCII "dose-file" for each plane in the resist volume. The "easy" rotation, R1, which represents a 90 degree rotation about the axis of the incident x-ray beam, simply involves interchanging "rows" and "columns" within each dose-file. The second rotation, R2, which represents a 90-degree rotation about an orthogonal axis, requires mixing among all of the dose-files representing the resist volume. With an appropriate mask, the sequence: exposure, R2, exposure, R1, R2, exposure produces a six-way cross. A CAD drawing of the basic geometry of the six-way cross is shown in figure 2.

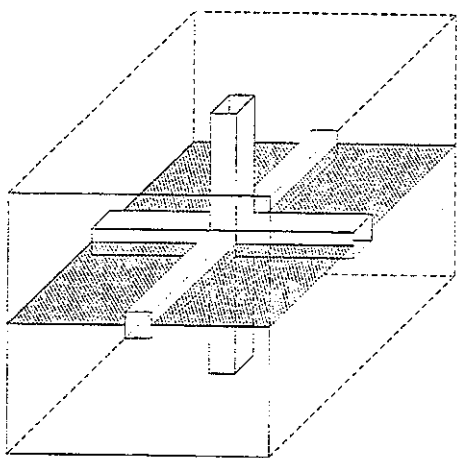


Figure 2: CAD drawing of the geometry of a six-way cross in a cube with a square cross-section.

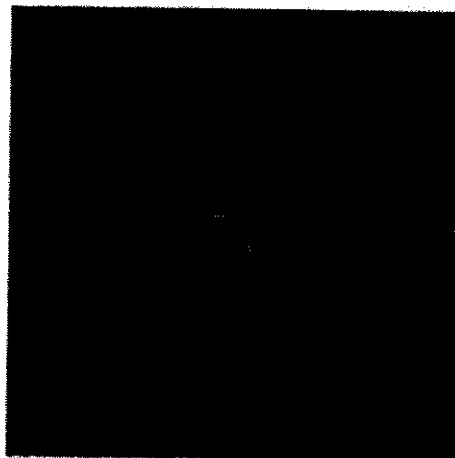


Figure 3: Dose distribution in the middle plane of the cubic volume after the first exposure in a setup using a square aperture.

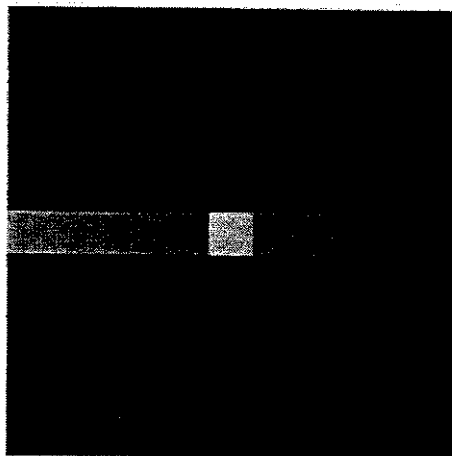


Figure 4: Dose distribution in the middle plane after R2 and the second exposure.

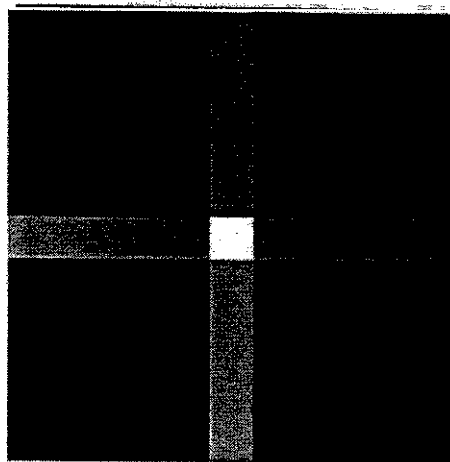


Figure 5: Final dose distribution. The six-way cross structure now is complete.

## Simulation Results

The six way-cross was simulated with a  $256 \times 256 \times 256$  resist volume of PMMA. Each voxel represented one cubic micron. A  $25 \times 25 \mu\text{m}$  square aperture in  $3.5 \mu\text{m}$  of gold on a  $2 \mu\text{m}$  silicon nitride carrier was used for the mask. A single x-ray energy of 4.4 keV was used. This x-ray energy was chosen to illustrate the variation of dose with depth in the resist. Monochromatic x-rays were used and diffraction effects turned off to minimize compute time.

The following pictures show cuts through the same plane located in the middle of the cubic volume. The horizontal plane is shown hatched in figure 2:

- Figure 3 shows the resist after the first exposure.
- R2 has been applied to the resist data and the second exposure leads to the dose distribution shown in figure 4.
- Figure 5 shows the final dose distribution after applying R1, R2 and the third exposure.

## First Experiments

Using the X-ray Ring in Brookhaven National Lab a six-way cross structure has been produced. Figure 6 shows a photograph of the cross in PMMA. A rod instead of a cube was used for easier mounting of the sample on the angular manipulator. The diameter of the rod was 10 mm and the aperture was set to  $500 \mu\text{m}$  square cross section. Figure 7 shows the used hardened spec-

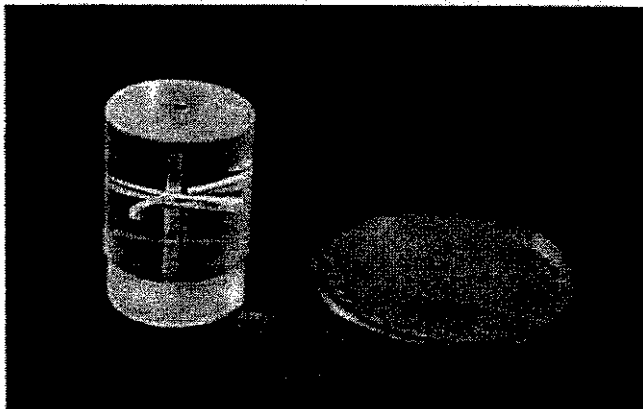


Figure 6: Picture of the six-way cross produced at NSLS hard X-ray Ring. The American Penny on the right is included to give a proportion scale.

trum of the X-ray Ring at a beam energy of 2.58 GeV with 310 mA of beam current. The experiments were done at beamline X27B with filters of 1 mm beryllium, 0.5 mm silicon and  $25 \mu\text{m}$  aluminum to eliminate low energies. Lower energies are not desirable because the low energy radiation cannot penetrate to sufficient depth

in the resist leading to an overdose in the top part of the material.

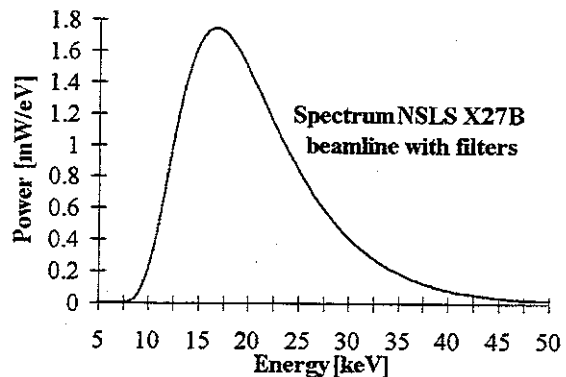


Figure 7: The spectrum of X27B beamline used for exposure of the six-way cross.

The desired rotations were achieved using a two axes goniometer mounted approximately 30 cm behind the synthetic aperture. The synthetic aperture was realized with a pair of vertical and a pair of horizontal tubes of titanium mounted on rotary stages [1].

Development has been done in an ultrasonic bath of MIBK at a constant temperature of  $30^\circ \text{C}$ . The MIBK concentration was 20%, thinned with ethanol. Development time was ca. 8 hours.

## THE VALVE SEAT

As a first example of 3-dimensional exposures with non-normal angles of incidence a valve seat has been chosen. It has the shape of a (negative) truncated pyramid with a square cross section. Figure 8 shows a CAD drawing of the valve seat structure.

Simulation of the exposure sequence to produce this valve seat used a resist volume that was represented by 50  $1 \mu\text{m}$  thick slices. Each slice was further subdivided by a  $300 \times 300$  grid yielding  $1 \mu\text{m}$  cubic voxels. The "non-normal incidence" aspect of the model was achieved by shifting layers following a normal-incidence dose calculation using the Toolset. When shifting layers, voxels on the leading edge of a layer were moved to the trailing edge of the layer. Thus, as with the six-way cross, the manipulations of the resist volume left the material properties unchanged. The result of the shifting operation is indicated schematically in Figure 9. The top layer has been shifted, in this figure, up by  $98 \mu\text{m}$  and to the left by  $98 \mu\text{m}$ . This distance is equal to the length of the diagonal of the aperture of the mask less  $2\sqrt{2} \mu\text{m}$ . The bottom layer of resist has not been shifted.

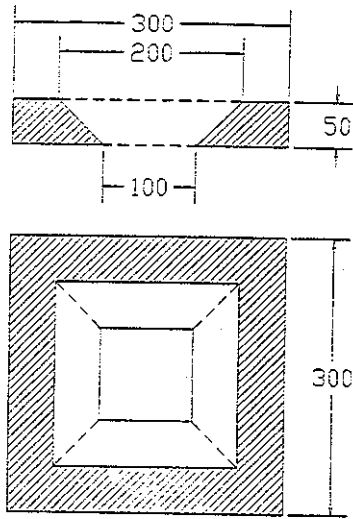


Figure 8: CAD drawing of the geometry of the valve seat to be simulated

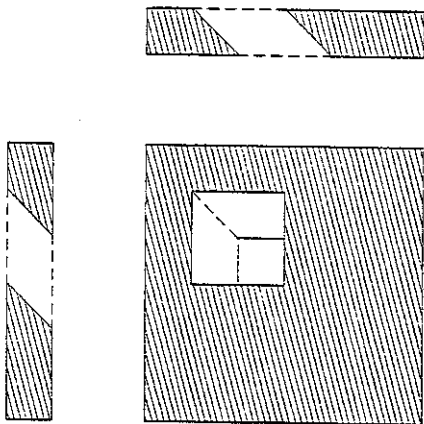


Figure 9: CAD drawing of the geometry after the first exposure producing a valve seat.

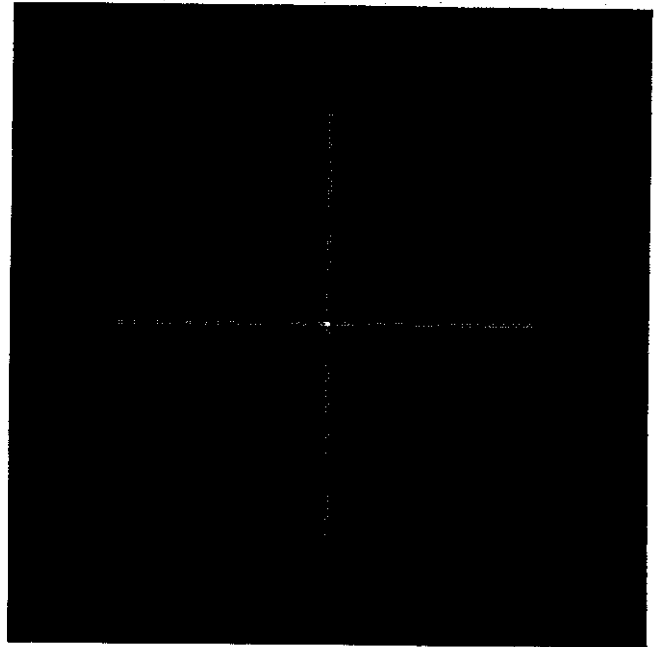


Figure 10: Dose distribution in the top layer of the resist producing a valve seat structure.



Figure 11: Dose distribution in a vertical cut through the resist volume in the middle of the resist (pixel 150).



Figure 12: Dose distribution in a vertical cut through the resist volume off center of the resist (pixel 125). One can see the four incoming beams and the single, double and fourfold doses in the cut.



Figure 13: Dose distribution in a vertical cut through the resist volume off center of the resist (pixel 75) where the sloped wall already begins. One can see the depth of the exposure ending sharply on the sloped wall.

When calculating the dose with the Toolset, the density of the resist was scaled by  $\sqrt{3}$  to achieve the correct dose per layer for the non-normal incidence model.

Figure 10 shows the calculated dose in the top layer of resist after four exposures and all necessary shifting operations. The exposures overlap by two voxels. Figures 11 - 13 represent slices through the resist normal to figure 10.

Figure 11 is a vertical slice through the middle of the device. The two downward-pointing triangles are regions where two exposures overlap. The upward point triangle is where four exposures overlap.

Figure 12 is a vertical slice 25  $\mu\text{m}$  away from figure 11. The two dark trapezoids at the top of the figure are regions illuminated by only one exposure. The three triangular regions are where two exposures overlap. The light trapezoid and the bottom of the figure is where four exposures overlap.

Figure 13 is 75  $\mu\text{m}$  away from figure 11. It intersects the sloping surface of the valve seat. The two dark trapezoids indicate illumination by one exposure. In the triangular region, two exposures overlap.

## COMPUTING REQUIREMENTS

The above simulations were performed on a 200 MHz Pentium system running Linux. The computer had 512k of L2 cache, 96 megabytes of ram, and an 8.4 gigabytes IDE disk. The  $256 \times 256 \times 256$  six-way cross utilized over 500 megabytes of swap space requiring five swap partitions.

Table 1: Calculation times for the different grid sizes and operations in seconds.

Operation	t(64)	t(96)	t(128)	t(192)	t(256)
expose 1	40	115	365	1406	3840
expose 2	67	180	540	1897	5284
expose 3	61	160	444	1784	4404
rotation 1	5	25	75	215	1063
rotation 2	27	69	206	876	1450
rotation 3	5	19	49	172	1448

A computationally significant result that can be extracted from table 1, can be found by comparing the rows for exposure 2 and 3. From the point of view of the Toolset, these calculations are equivalent. The important difference is in the number of digits representing the dose for each voxel in the input dose-file. The native ASCII dose-file output format of the Toolset provides 15 digits of significance to the right of the decimal place. The rotations between exposure 2 and 3 specifically limi-

ted this number to 6. The number of digits to the right of the decimal point was typically 6 or 7. Approximately 15% of t(256) for exposure 2 was due to digits 7 thru 15 to the right of the decimal place in the input dose-files. The most important performance improvement will be to write and read all of the intermediate dose-files in binary format. A decrease in exposure simulation time of at least a factor of two is anticipated.

Probably the next most important deficiency of the present approach is the fact that a "materials" (.mm) file is read in for each plane of the resist. A "short-circuit" method of informing the Toolset that all slices within the resist share the same material properties would save significant execution time. Besides saving the time required to read these binary files, a very significant decrease in the demand for swap space would be realized.

The incorporation of the resist manipulations into the Toolset itself will be the final step in this sequence of optimizations.

## FUTURE DIRECTIONS

The preliminary simulations presented here demonstrate some basic capabilities of simulating 3-dimensional lithography problems using the CxRL Toolset. Such calculations support planning deep x-ray, precision machining exposure scenarios.

In the near term, a mask will be produced for the valve seat. This mask will be qualified using the white-light Micromachining III beamline at CAMD [3].

A superconducting wiggler will be installed at CAMD this year [4]. A versatile 3-D, deep x-ray exposure station for a wiggler beamline is under development. The six-way cross will be one of the mechanisms used to align and characterize the exposure system. This system will then be used to produce a prototype valve seat.

## CONCLUSIONS

The CXrL Toolset can definitely be used for simulations of some classes of 3-D, deep x-ray lithography exposures. These simulations can provide important insight into the evolution of the dose distribution during a series of exposures. The most important deficiency in the approach described in this paper is the ASCII file method used to communicate dose distributions between the Toolset and the external programs that manipulate the resist volume.

In the future it will be important and necessary to quantitatively compare simulation results with experimental data.

## ACKNOWLEDGEMENTS

We would like to thank Mumit Khan and Franco Cerrina from the University of Wisconsin-Madison for giving us access to the source code of the CXrL Toolset and assistance in installing it. Our thanks also goes to NSLS Brookhaven for beamtime at X27B. Special thanks to Peter Siddons and his R&D group who supported our experiments and let us use their equipment.

## REFERENCES

- [1] E. Johnson and C. Milne, "A hard X-ray Prototype Production Exposure Station" (BNL Pub 64629), To be published in *Microsystems Technologies*.
- [2] M. Khan and F. Cerrina, "CXrL Toolset User's Guide", University of Wisconsin-Madison, 1996.
- [3] Y. Vladimirovsky, K. Morris et. al. "X-ray exposure system for induced chemistry and dry processes in microlithography", *Journal of Vacuum Science & Technology B* Vol. 13 No. 6 (p. 3109) 1995.
- [4] N. Mezentsev, B. Craft, et. al., "Superconducting 7 Tesla wiggler for LSU CAMD", To be published in proceedings of SRI 97.